# FATIGUE BEHAVIOR OF COLD SPRAY-COATED ACCIDENT TOLERANT CLADDING

M. ŠEVEČEK[a,b], J. KREJČÍ[a],
[a]*Faculty of Nuclear Sciences and Physical Engineering, Czech Technical University in Prague*
*Břehová 7, Praha 1, 115 19, Czech Republic*
M. H. SHAHIN[b], J. PETRIK[b], R. G. BALLINGER[b], K. SHIRVAN[b]
[b]*Department of Nuclear Science and Engineering, Massachusetts Institute of Technology*
*77 Massachusetts Ave, Cambridge, MA, 02139, USA*

## ABSTRACT

The Zircaloy cladding is subjected to oscillating loads during normal operation in Light Water Reactors (LWRs). Crack initiation and growth due to vibrations and pressure variations in fuel cladding can jeopardize its integrity and might lead to plant downtime costs and safety concerns. Coated claddings are considered a near-term Accident Tolerant Fuel concept, where the primarily goal is to protect the Zircaloy substrate with a corrosion-resistant coating. Therefore the fatigue behavior of the coating is crucial in its ability to protect the base Zircaloy material as crack initiation and growth in the coating could lead to exposure of the Zircaloy to the reactor coolant. Of particular interest, the fatigue behavior of cold spray coated Zr-based alloys has not been studied in detail. The cold-spray technique can substantially affect the substrate and its properties at the interface which brings new questions to the problem of fatigue behavior in the bulk material. In this work, fatigue behavior of Zr-based alloy coated with FeCrAl, Cr, and Mo by cold spray was studied at room temperature and NWC environment. The experimental system is described and preliminary results are presented. The behavior of the reference uncoated case (pure Zircaloy-4) is also compared to the coated materials.

## 1 Introduction

Accident Tolerant Fuels are defined as nuclear fuels that can tolerate severe accidental conditions in an LWR for a considerably longer time compared to reference fuel system while maintaining or improving fuel performance in nominal operating conditions, AOO and postulated accidents [1]–[5]. One of the evolutionary approaches to ATF cladding is to deposit a protective coating on a surface of the standard Zr-based cladding material (a substrate). The standard Zr-based materials have been utilized as a nuclear fuel cladding materials in Light Water Reactors (LWRs) for decades and will still serve as the main structural component of the coated clad concept.

The oscillating loads in a reactor caused by vibrations and pressure variations in fuel cladding can lead to crack growth. This can generally jeopardize cladding integrity and might lead to downtime costs and safety risks. It is therefore of interest to determine fatigue crack growth threshold and fatigue crack growth rate data in the threshold region for different material-environment systems. These data are needed to estimate the remaining life of components, to determine the time between inspections, and for safety analysis. The particular conditions under which a flaw may be initiated or grow to the critical size resulting in unstable fracture are important in the design of fuel rods and assemblies and are part of the design basis. The applied safety factor is typically based on the stress amplitude or the number of cycles whichever is more conservative. Factors that can have an influence on the measured fatigue crack growth threshold for a specific material are: the environment, load frequency, load ratio, and rate of stress intensity factor reduction in the test [6], [7].

It has been reported that the coatings will have limited impact on the neutronic performance of LWR cores if thin enough [8], the thermo-hydraulic performance depends on the particular surface conditions and its treatment but it can potentially enhance the behavior of the cladding in comparison with the reference case [9]. Some of the coatings improve also the behavior at the accidental condition, namely high-temperature oxidation, post-quench ductility, ballooning

and burst, or hydrogen pickup [10]–[14] and they also enhance wear resistance, corrosion and consequent hydrogen pickup [11], [12], [15]. Coatings can be beneficial also in the backend of nuclear fuel cycle when manipulating, storing or disposing of the spent nuclear fuel due to enhanced ductility.
The coatings can be deposited by various techniques – chemical vapor deposition, physical vapor deposition, laser deposition, thermal spray, atomic layer deposition etc. [14], [16]–[19]. Every deposition technique entails certain characteristics and affects the behavior of the coating and substrate in a different way. As was shown earlier, the cold sprayed coatings can substantially affect, deform or harden the surface of a substrate [11], [16]. This effect is very obvious when depositing hard materials (e.g. pure Cr) on a softer substrate. The deposition leads to plastic deformation of a coating but also the substrate at the interface. As mentioned, the Zr-based substrate keeps its structural function in the multicomponent cladding. If the surface is deformed by the coating, the behavior of the substrate might change including its structural characteristics and strain fatigue. For that reason, fatigue behavior of cold sprayed materials was studied in air and Normal Water Conditions (NWC) [20].
Fatigue testing is a standard part of fuel rod design, however, most of the data are proprietary. Limited data on an influence of different factors on the lifetime and fatigue strength of some of the Zr-based alloys - Zircaloy-4 [21]–[24] , E110 [25] and E125 [26] are available. There are ongoing studies of fatigue testing of multicomponent cladding at KAERI [27] but the results have not yet been published. Results of fatigue testing of different coated materials [28]–[31] suggest that the fatigue behavior is case specific and that the data cannot be extrapolated for different conditions or deposition techniques [28], [30], [31]. For that reason, an experimental system for fatigue testing was designed and will be utilized for more complex testing in future.

## 2 Experimental setup

### 2.1 Materials

Standard commercially available Zircaloy-4 was used as a substrate for all tests. Three different coating materials were deposited by the cold spray technique – pure Cr, FeCrAl – low alloy; pure Mo. The fundamental physical and material properties of the materials of interest at room temperature are summarized in Table 1. Uncoated Zircaloy-4 was also studied as the reference case after cleaning in DI water, ethanol and acetone in agreement with [32].

Table 1: Bulk material properties of tested materials at RT [33]–[37]

| | **Zircaloy-4** | **Chromium** | **FeCrAl LA** | **Mo** |
|---|---|---|---|---|
| Crystal structure | hcp | bcc | bcc | bcc |
| Thermal $\sigma_a$ [barn] | 0.2 | 3.03 | 2.43 | 2.65 |
| Density [g/cm$^3$] | 6.56 | 7.19 | 7.3 | 10.22 |
| Hardness [HV10] | 275 | 250 | 200 | 220 |
| Specific heat capacity [J/g-C] | 0.285 | 0.461 | 0.46 | 0.255 |
| Thermal conductivity [W/m-K] | 21.5 | 93.7 | 11 | 138 |
| CTE [µm/m-C] | 6.00 | 6.2 | 11.2 | 5.35 |
| Poisson ratio [-] | 0.37 | 0.21 | 0.28 | 0.32 |
| Young's modulus [GPa] | 97.5 | 279 | 195 | 330 |

The FeCrAl low alloy (FeCrAl LA) composition in weight percentage is Fe-10Cr-6Al. Different thicknesses of FeCrAl coatings were used and also different grinding or polishing processes were used before testing. Pure molybdenum was deposited on the substrate as confirmed by XRD after deposition. The Mo coatings in as-polished condition were much thinner in comparison with the FeCrAl coatings and there were even defects observed by optical microscope. There are two series of samples for which the rolling and transverse direction of the substrate are opposite. The as-coated and cleaned samples are shown in Fig. 1.

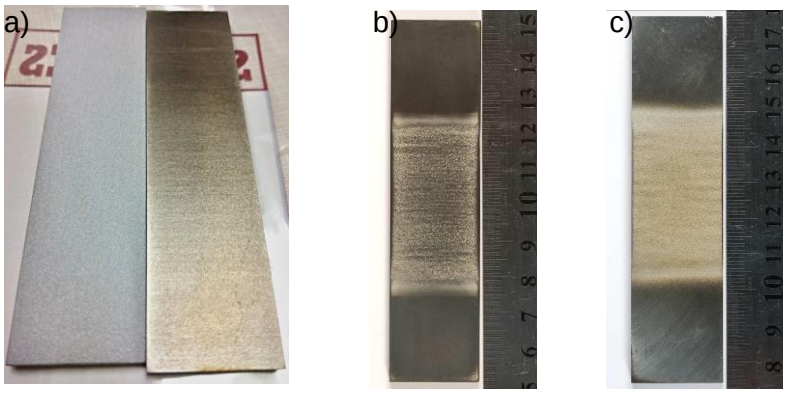


Fig. 1: As-coated and cleaned samples - a) Chromium CS coated and uncoated Zry-4 sample, b) Mo CS coated sample, c) FeCrAl LA coated sample

The SEM micrographs in Fig. 2 show the top view on the Cr and FeCrAl LA coated samples. The left image shows the interface between Cr coated and uncoated Zircaloy-4. The Cr coating is more plastically deformed in comparison with the FeCrAl LA coating shown on right where single particles and their size are visible. Both of them were deposited using a different system with different deposition parameters which affects also an appearance of the coatings.

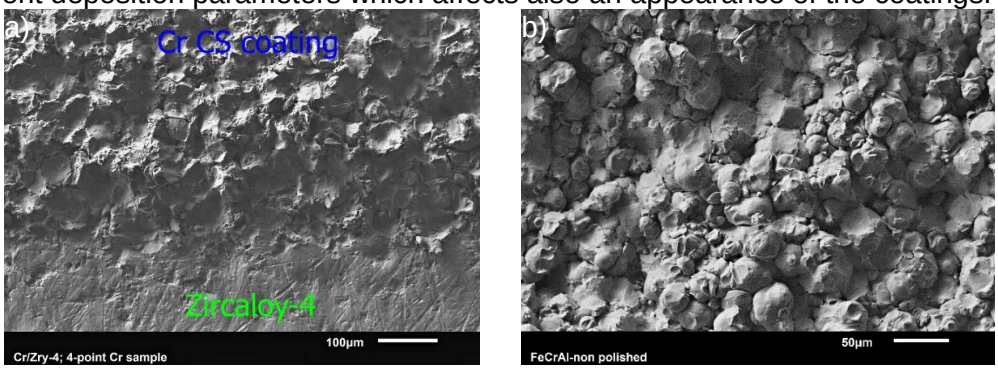


Fig. 2: SEM micrograph of the as-coated and cleaned bending samples (top view) in SE mode: a) Cr CS coated Zircaloy-4 and b) FeCrAl CS coated Zircaloy-4

As mentioned, there were two environments in which the materials were tested – air at room temperature and DI water between 300-312°C (Normal Water Conditions). It was found that Mo quickly corrodes in NWC conditions and creates volatile Mo-oxide which is then washed away by the hot water. The EDX linescan on the SEM micrograph in Fig. 3 shows the Mo coated Zircaloy-4 after short-term exposure to NWC environment. The Mo coating is gone and only traces caused by the Mo particles interaction with the substrate during CS process are visible. For that reason, Mo coated samples were tested in air at room temperature only.

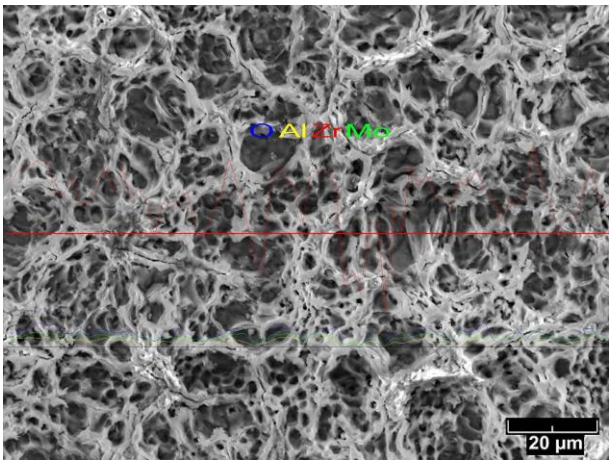

Fig. 3: EDX analysis of the Mo coated Zircaloy-4 exposed to NWC environment

## 2.2 Cold Spray Process

All tested samples were coated using the cold spray process (CS). It involves the acceleration of micron-sized particles in the form of powders that are carried in a high pressure and sometimes heated gas stream (room temperature (RT) – 1200°C) in the solid state toward a suitable substrate.

### 2.2.1 Process Parameters

Two commercial CS systems were utilized to deposit coatings for fatigue testing. VRC Gen III system at ARL, MA was used to deposit chromium coatings and CGT Kinetiks 400/34 system at University of Wisconsin was used to produce FeCrAl and Mo coatings.
The VRC Gen III was operated using helium as the accelerating gas. The feedstock powder was pure chrome with an average particle size of 44 µm, an oxygen content of 600 ppm and a nano-hardness value of 5.1 GPa. A De Laval tungsten carbide nozzle with a circular exit with a 1.75 mm throat, a 5 mm exit, with a 152 mm expanding length and a 10° converging section was used. The remaining process conditions can be found in [11].

To deposit FeCrAl and Mo coatings a commercial cold spray system (CGT Kinetiks 400/34 unit) and a six-axis industrial robotic system at University of Wisconsin-Madison were utilized [16]. FeCrAl alloy powders were manufactured by gas atomization. Mo powders (99.8 wt.% purity) were manufactured by the spheroidization process. Cold spray deposition was performed on Zry-4 substrate using nitrogen as the accelerating gas. Process parameters such as gas preheat temperature and gun translation speed were optimized to improve the microstructure, deposition rate, and coating-substrate adhesion and the details of the process can be found in [38].

## 2.3 Experimental Setup

The designed experimental setup for fatigue testing can be divided into several parts according to their functions and position in the system. The parts of the experimental setup are:

- Water loop - control of water chemistry (pH, conductivity, cleaning, hydrogen, boron, Li), circulation of water (flow rate), preheating, pressure control.
- Autoclave - seals the bending setup in the environment controlled by water loop, heating of the environment, temperature control. It is a dynamic autoclave with continuous water exchange. The autoclave with the water loop in the back is shown in Fig. 4.

Fig. 4: Dynamic autoclave with its heater connected to the water loop.

- Bending setup - in-house made 4-point bending system based on ASTM standard for measurements of the flexural strength of advanced ceramics [39]. The bottom part of the setup is connected by the pull rod to the Instron machine. The top part is fixed and stabilized. There are bearings used in order to stabilize the sample in the central position and to compensate for the thermal expansion and deformation of the setup.
- DCPD system - potential drop measurement system based on ASTM standard for fatigue growth measurements [40]. The technique involves passing a constant current through the test piece and accurately measuring the electrical potential across the crack plane. As the crack propagates, the measured PD increases due to the reduction in the uncracked sectional area of the specimen. Schematics of the bending setup with the connected DCPD system is shown in Fig. 5.
- Instron - standard Instron 8500 machine that is operated in the load control mode with a sine wave of various frequencies.
- Data acquisition systems –separate systems for collection of: 1) DCPD data; 2) load, number of cycles and displacement data; and 3) water loop data (pH, water conductivity, ECP, flow rate, oxygen and hydrogen concentration).

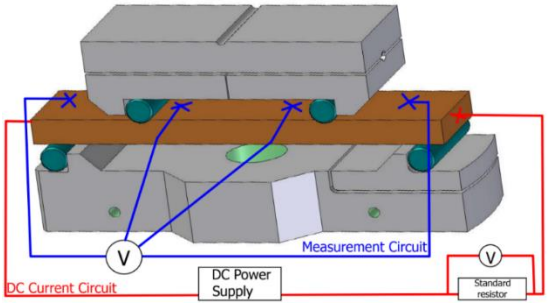

Fig. 5: Schematics of the bending setup made of SS (grey) with ceramic pins (green) and reference sample (brown). The DCPD consisting of DC current circuit and measurement circuit is connected the sample by spot welding.

## 2.4 Testing procedure

As-coated samples were first ultrasonically cleaned in water, DI water, acetone and ethanol before testing. Pt probes were then welded on the edges (DC current circuit) and the top surface of the sample (measurement circuit) by spot welding.

The sample is then placed into the bending setup and fixed by bearings and ceramic pins in its position. The probes are connected to the DCPD system which is then tested. The setup is enclosed by the autoclave which is filled with water and pressurized. The water loop then circulates cold water inside the system until the required environment is reached (gas/liquid bubbling, cleaning). The system is heated to required temperature and bending starts once the conditions are stable. Data acquisition systems are monitoring environment, loading sequence and the sample. The procedure is summarized in Fig. 6 a) to f).

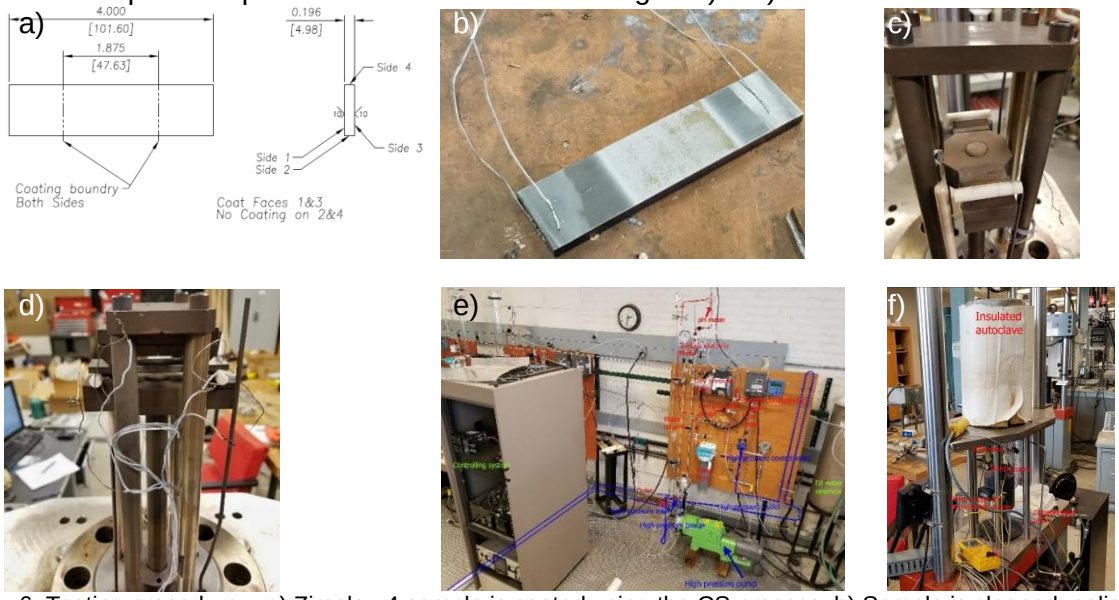


Fig. 6: Testing procedure – a) Zircaloy-4 sample is coated using the CS process; b) Sample is cleaned, polished and Pt probes are welded on the surface; c) Bending setup is assembled and balanced; d) Sample is placed into its position and connected to the DCPD system; e) Bending setup is enclosed in the autoclave, filled by DI water and pressurized; f) When the required environment is reached (heatup, chemistry control) bending is initiated using the Instron machine

All the tests were performed in the load-control mode with the load of 20 - 1800 N defined by a sine wave with the frequency of 3-4 Hz. The minimal value of 20 N during the cycle was used to keep the sample in its fixed position. The bottom surface of the sample was under tension and the top surface under compression. As the test was running in load control mode, the mean displacement shifted during the test to keep the load constant and to compensate for cracking, plastic deformation and creep. The displacement was recorded as a supplement to DCPD results.

## 3 Results

Testing was done in two different environments – air at RT and NWC environment between 300 and 312°C. Conditions of one of the NWC test are summarized in Fig. 7. The first graph shows temperature and pressure inside the autoclave during the test. The fatigue testing was performed in this case between 6-19 hours of presented elapsed time when the conditions are very stable and close to required values (ECP, water conductivity, pH and oxygen concentration).

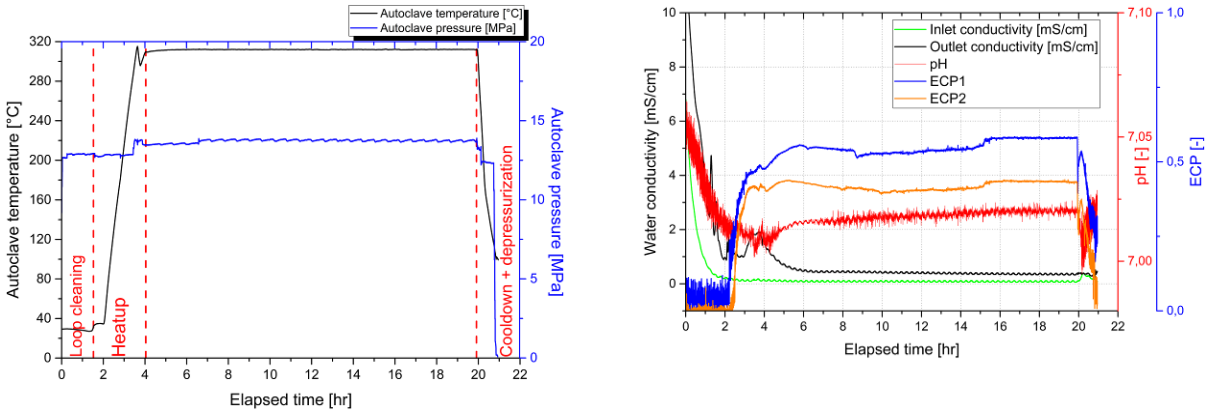


Fig. 7: The standard environment for tests in NWC conditions. These are the particular conditions for the test with the uncoated Zr-BS3 sample but the environment for other high-temperature tests was similar.

The DCPD data from testing in NWC conditions are summarized in Fig. 8 up to 200,000 cycles. Some of the tests continued up to 900,000 cycles. However, it was found that due to high-temperature creep, the samples bent and the values above 300,000 cycles were not representative. The solution for creep reduction would be to increase the frequency, decrease the load or both. The frequency is limited by capabilities of the Instron machine and lower loads would lead to extremely long testing times. Therefore, a compromise between the frequency and the load was made based on the initial test findings.

The initiation and slow growth of cracks is clearly visible from the data DCPD data shown in Fig. 8. It can be seen that PD increased for Cr coated sample first which corresponds to the early initiation of cracks. Number of cracks initiated from the coated surface and their growth quickly continued during the test. On the other hand, the crack was initiated much later for the FeCrAl coated sample. However, the growth was much faster because there was one main damage site and not many sites as in the case of Cr coated samples. It should be noted that the FeCrAl coating presented in the results was thicker compared to Cr coating. Initiation of cracks for uncoated Zry-4 was observed later and also the crack growth was slower than for coated samples. The second test with the uncoated sample was stopped due to leakage in the system but the sample reached more than 500,000 cycles with only minor failures.

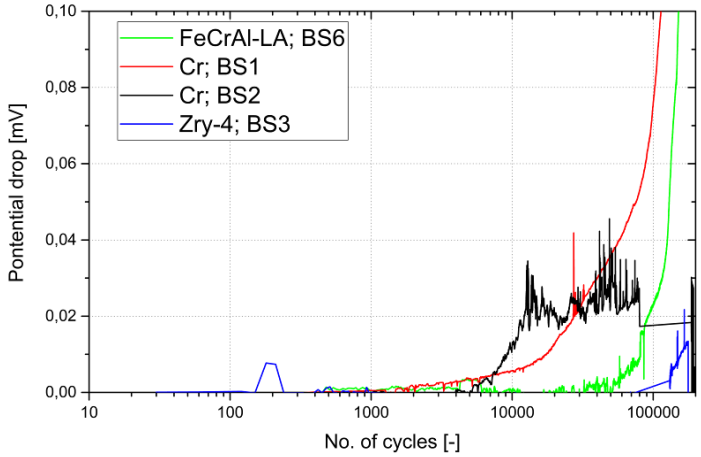


Fig. 8: Potential drop measurements for FeCrAl and Cr coated samples in comparison with reference Zry-4 sample in NWC conditions. Fatigue life of coated materials is reduced.

The mean value of the displacement was recorded during testing and the shift which directly shows different behavior of the samples was calculated. Fig. 9 shows the results of the mean

displacement shift that was recorded every ten seconds and every value represents the displacement during one sine cycle.
The plot confirms early cracking of the Cr coated samples in comparison with uncoated reference samples as measured also by the DCPD. The test with Zry-4, BS2 reached more than 500,000 cycles and then was interrupted. The simulation using the Bison code in [41] predict higher stresses in coatings and substrate in comparison with the reference case during normal operation of an LWR mainly due to mismatch in CTE and creep properties. These additional stresses inherent to CS coated materials lead also to premature cracking shown in the plot. The second effect that plays a role is the behavior of the material is the nonhomogeneous nature of the CS coatings. This could lead to non-uniform stress distribution and stress concentration. As a result, the cracks initiate easier in comparison with the uncoated cladding.

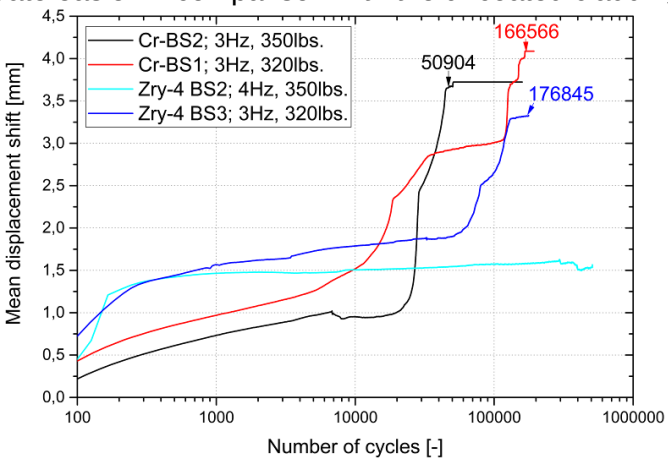


Fig. 9: Mean displacement shift during the test. It shows higher plastic deformation/relaxation of uncoated Zircaloy-4 samples. The Cr-coated samples deform slowly up to a point when cracks are initiated.

## 3.1 Uncoated Zircaloy-4

Three reference uncoated Zircaloy-4 samples were tested. The appearance of the third sample before and after the test is shown in Fig. . The sample (similarly to other tested at high temperature) bent during the test due to high-temperature creep. It is obvious also from the crack propagation shape visible in the side-view on the sample. The crack propagates perpendicularly to the maximal stress direction that changed after sample crept under the load.

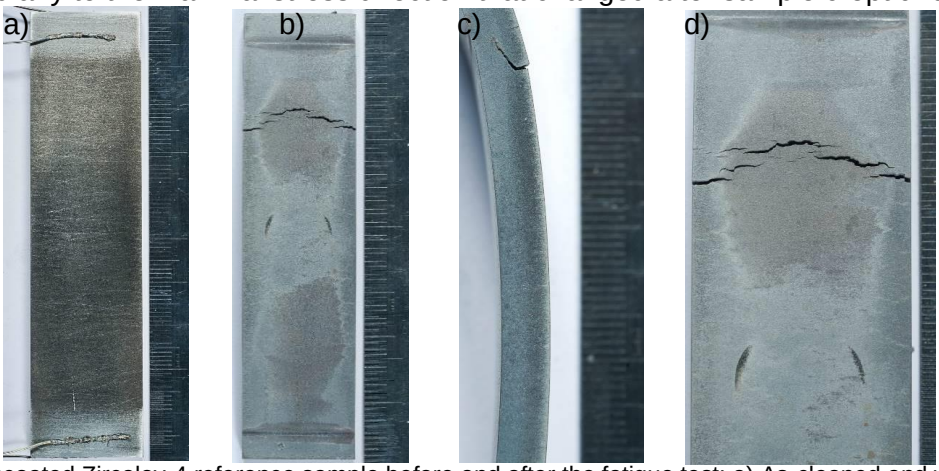


Fig. 10: Uncoated Zircaloy-4 reference sample before and after the fatigue test: a) As-cleaned and welded sample before testing; b) Bottom surface under tension after the test; c) Side view with the detail of the crack growth direction; d) Main crack on the bottom surface.

There were small cracks detected on the side of the plate that underwent tension. The stress between the ceramic pins of the setup is uniform and without a notch or other stress concentrator at the surface, the cracks will initiate randomly. In reality, the cracks initiated in the bending location similarly to the Zry-4 sample shown in the previous figure. The fracture surfaces shown in Fig. 11 show mostly ductile behavior due to testing at high temperature but fatigue striations are also visible.

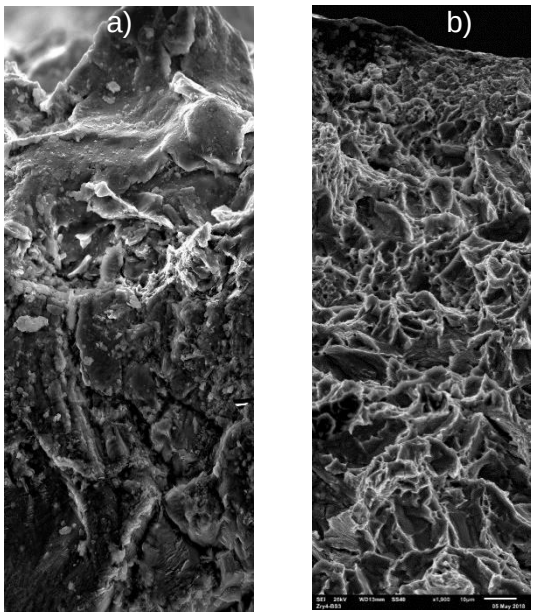


Fig. 11: Fracture surfaces of the fatigue tested a) Cr-coated Zircaloy-4 at NWC conditions and b) Uncoated Zicaloy-4.

## 3.2 Cr-coated material

Two Cr-coated samples were tested in NWC environment. During the first experiment, a high-pressure seal partially failed and the system was losing its coolant. The water was continuously refilled but its quality was not adequate and there was no time for additional cleaning and precise chemistry control. Therefore the conditions during the test changed rapidly (except temperature and pressure) which affected mainly corrosion of the material which is obvious also the visual evaluation.

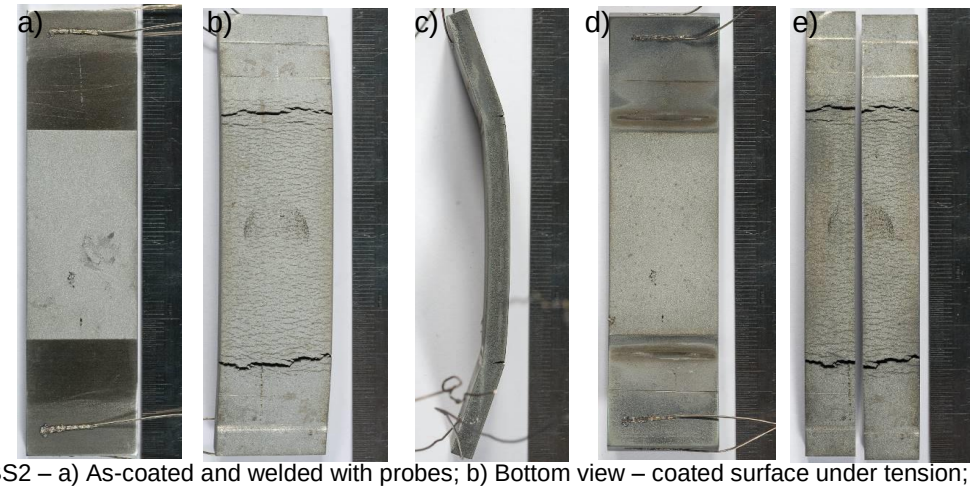


Fig. 12: Cr-BS2 – a) As-coated and welded with probes; b) Bottom view – coated surface under tension; c) Side view after the test – reduced creep in comparison with Zry-4; d) Top view - coated surface under compression; e) Longitudinal cut for crack analysis.

The Cr-coated samples were fully coated on one side of the sample and partially coated on the other – between the pins only as can be seen in Fig. 12 and 14. The fully covered bottom surface was under tension and the top surface under compression. There were no defects observed on the top side and the coating was fully adherent after the test. There were many cracks on the bottom surface and the sample failed at the location of the pins.
The SEM micrograph shown in Fig. 13 shows on the cracks initiated in the central area of the sample. The cracks initiated from the Cr coating grow further to the Zry-4 substrate up to hundreds of microns.

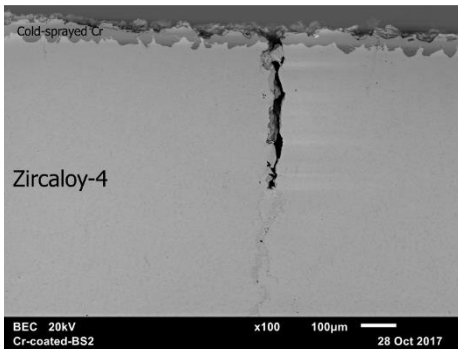


Fig. 13: SEM micrograph in BEC mode of the Cr-BS2 sample cross section after the test. The Cr coating is non-homogeneous and its thickness is between 10-65 µm. The coating is adherent but its cracking initiated cracks also in the substrate. There are many similar cracks in the coating visible after the test.

The behavior of second Cr coated sample is similar to the first sample. The growth was slightly affected by accelerated corrosion but the resulting fatigue behavior is comparable.

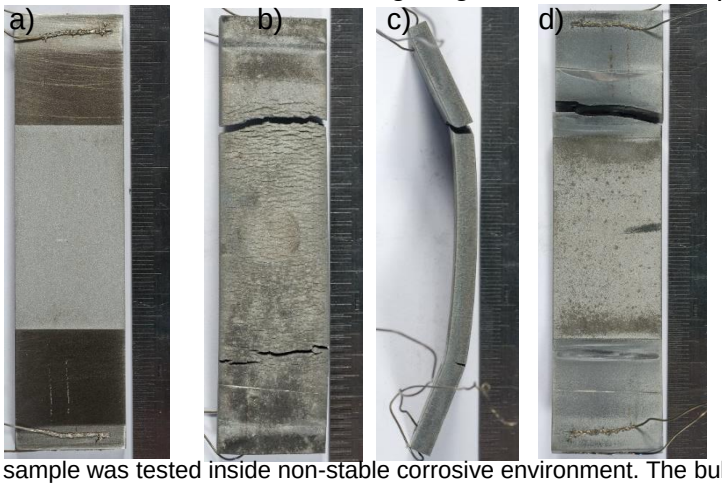


Fig. 14: Cr-BS1 – the sample was tested inside non-stable corrosive environment. The bulk behavior is comparable to the BS2 sample but the corrosion changed drastically. a) As-cleaned and welded sample; b) Bottom surface under tension after the test; c) Side view with the shape of the crack; d) Top surface under compression during the test.

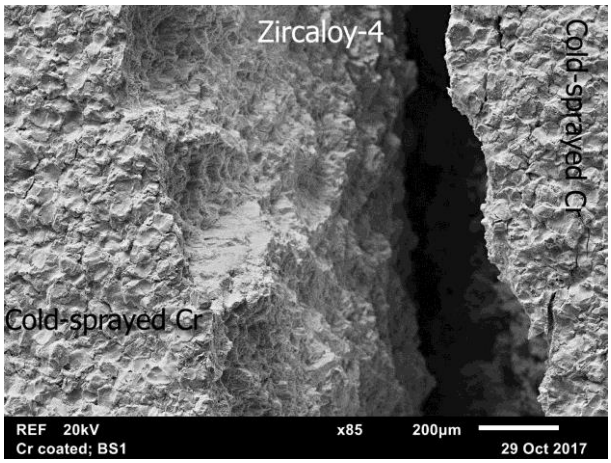

Fig. 15: SEM micrograph of the fracture surface of the Cr coated Zircaloy-4.

## 3.3 FeCrAl coated material

The thickness of as-coated FeCrAl was much higher than Cr. The material was therefore effectively thicker in the coated region. The coating on the top surface under compression cracked and even spallation was obvious on the surface under tension. The coating also corroded which in combination with applied load was the reason for spallation which can be seen also in Fig. 16.

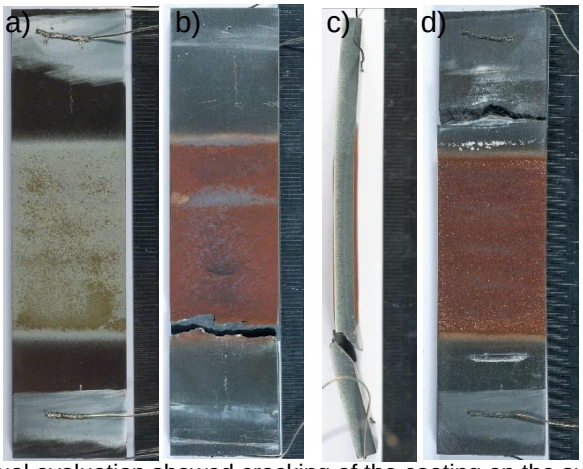

Fig. 16: FeCrAl-BS6 – visual evaluation showed cracking of the coating on the surface under compression and spallation of coating on the surface under tension. The creep of the coated section is reduced due to high thickness of the coating.

## 3.4 Mo coated material

As mentioned, Mo coated samples were tested in air at room temperature only. Due to lower temperature the sample is more brittle. It was found that cracks initiate from the welding spots that damage the surface and act as the stress concentrators. Later, the probes were welded far from the coated area. Figure 17 shows the appearance of the Mo-coated sample before and after fatigue testing.

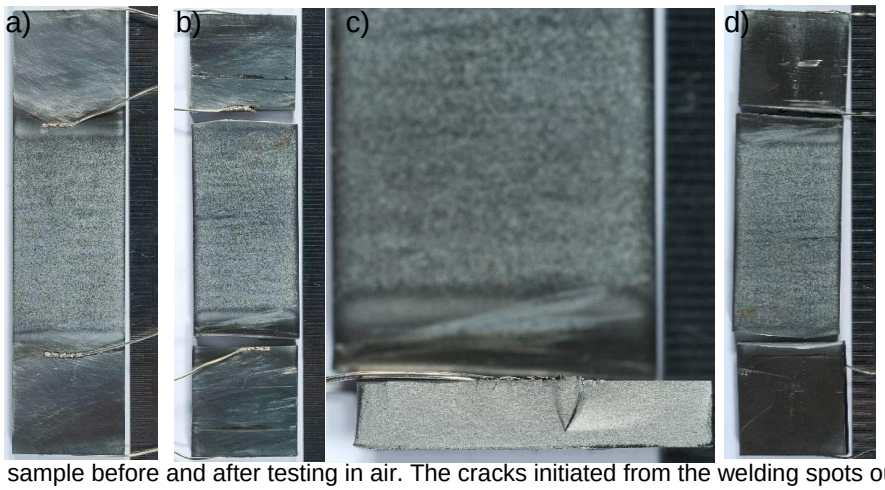


Fig. 17: Mo coated sample before and after testing in air. The cracks initiated from the welding spots out of the coated region. a) As-cleaned and welded Mo-coated sample; b) Top surface under compression; c) Fracture surface with the effects of welds; d) Bottom surface under tension.

Due to testing at the lower temperature, the crack growth is faster in comparison with the testing at high temperature once the crack is initiated. There were no major differences between the behavior of Mo-coated and uncoated Zry-4 samples at the room temperature observed because the crack growth is faster at room temperature and also the thickness of the Mo coating was low. On the other hand, the FeCrAl coating rapidly increased the fatigue life up to more than 2 million cycles as shown in Fig. 18.

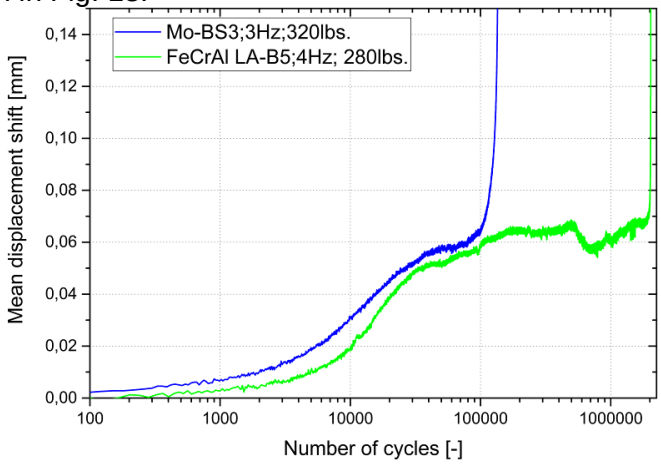


Fig. 18: Mean displacement shift for Mo and FeCrAl coated samples tested in air at room temperature. Mo-coated sample is very similar to uncoated Zircaloy-4. FeCrAl coating drastically enhances fatigue life in this case.

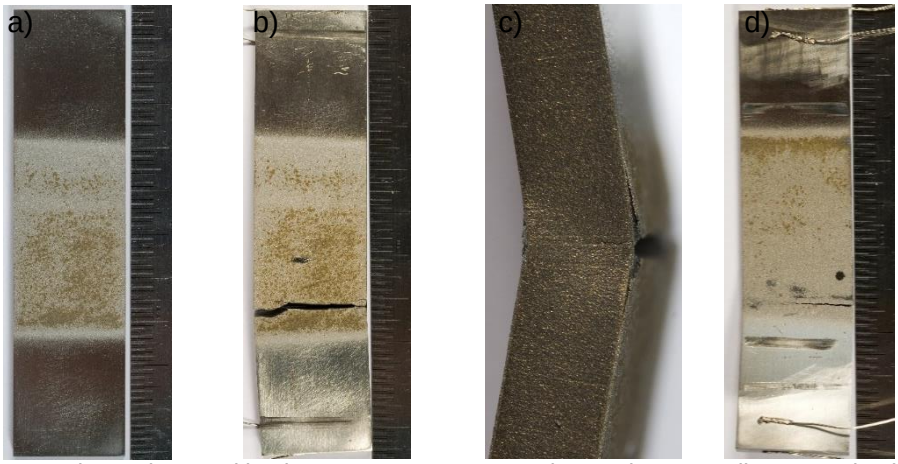

Fig. 19: FeCrAl LA coated sample tested in air at room temperature. The coating was adherent and enhanced fatigue life of the material. Cracking of the coating is visible only in the area of the cracked region.

## 4 Conclusions

The fatigue behavior of CS materials that are potential candidates for ATF cladding was studied. Standard Zircaloy-4 was used as a substrate and three different coatings were deposited on its surface by two industrial systems. To study the fatigue behavior, an experimental setup based on ASTM standards was designed and build. The setup was build inside an autoclave so the tests can be performed also in high-temperature and high-pressure conditions.

The design is based on the standard for testing of advanced ceramics and the DCPD technique was chosen for crack initiation and growth measurement. However, these methods have not been established for the geometry of the tested samples. Therefore modeling using the COMSOL Multiphysics code was used to optimize the system and its design. After the system was built, initial experiments showed some disadvantages and issues such as welding of probes, environment control and customized geometry of the sample and the setup. The experiment was tuned and first tests in air and high-temperature water were performed. It was found that Mo has a very poor corrosion resistance and therefore the tests with Mo coated materials were performed in air only.

A standard environment similar to NWC conditions of BWR reactors was defined for high-temperature tests and was controlled by the water loop. The experiments in the NWC environment showed that cracks might initiate earlier for coated materials in comparison with the reference uncoated case. The premature crack initiation may be related to stress concentration in the coating due to the inhomogeneities created by the CS process in this study. The fracture analysis showed the fatigue and plastic deformation mechanisms of the substrate and the characterization revealed the different behavior of coated materials. Previously it was reported that cold spray leads to an improvement in fatigue properties if a compressive residual stress in induced [31] but the presented results of Zr-coated materials suggest the opposite which might lead also to the reduction in the fatigue life of the coated components. Therefore a more comprehensive assessment of fatigue characteristics of the coated cladding concept needs to be done with different CS parameters and other coating techniques to quantify its impact on margin to fatigue failure.

**Acknowledgements**

The support for this work was provided by the US Department of Energy Integrated Research Project (IRP) Grant: DE-NE0008416. Chrome-Coated samples were provided by Victor Champagne (ARL), Matt Siopis (UTRC), and Aaron Nardi (UTRC). Molybdenum and FeCrAl-Coated samples were provided by Kumar Sridharan and University of Wisconsin IRP collaborators.

# 5 References


[1] L. Braase, “Enhanced Accident Tolerant LWR Fuels National Metrics Workshop Report,” Idaho National Laboratory (INL), INL/EXT-13-28090, Jan. 2013.

[2] J. Carmack, F. Goldner, S. M. Bragg-Sitton, and L. L. Snead, “Overview of the U.S. DOE Accident Tolerant Fuel Development Program,” Idaho National Laboratory (INL), INL/CON-13-29288, Sep. 2013.

[3] B. Hallbert and K. Thomas, “Light Water Reactor Sustainability Program Advance,” Idaho National Laboratory (INL), 2013.

[4] S. Bragg-Sitton, “Development of advanced accident-tolerant fuels for commercial LWRs,” *Nucl. News*, vol. 57, no. 3, p. 83, 2014.

[5] M. Sevecek and M. Valach, “Evaluation Metrics Applied to Accident Tolerant Fuel Cladding Concepts for VVER Recators,” *Acta Polytech. CTU Proc.*, no. 4, pp. 89–96, 2016.

[6] R. Bucci, “Development of a Proposed ASTM Standard Test Method for Near-Threshold Fatigue Crack Growth Rate Measurement,” in *Development of a Proposed ASTM Standard Test Method for Near-Threshold Fatigue Crack Growth Rate Measurement*, 1981.

[7] W. H. Bamford, “Application of Corrosion Fatigue Crack Growth Rate Data to Integrity Analyses of Nuclear Reactor Vessels,” *J. Eng. Mater. Technol.*, vol. 101, no. 3, pp. 182–190, Jul. 1979.

[8] I. Younker and M. Fratoni, “Neutronic evaluation of coating and cladding materials for accident tolerant fuels,” *Prog. Nucl. Energy*, vol. 88, pp. 10–18, Apr. 2016.

[9] J. Kang, T. K. Kim, G. C. Lee, M. H. Kim, and H. S. Park, “Quenching of candidate materials for accident tolerant fuel-cladding in LWRs,” *Ann. Nucl. Energy*, vol. 112, pp. 794–807, Feb. 2018.

[10] J. Bischoff *et al.*, “AREVA NP’s enhanced accident-tolerant fuel developments: Focus on Cr-coated M5 cladding,” *Nucl. Eng. Technol.*, vol. 50, no. 2, pp. 223–228, Mar. 2018.

[11] M. Ševeček *et al.*, “Development of Cr cold spray–coated fuel cladding with enhanced accident tolerance,” *Nucl. Eng. Technol.*, vol. 50, no. 2, pp. 229–236, Mar. 2018.

[12] J. Krejci, M. Sevecek, and L. Cvrcek, “Development of Chromium and Chromium Nitride Coated Cladding for VVER Reactors,” *2017 WRFPM*.

[13] J. Brachet *et al.*, “Behavior under LOCA conditions of Enhanced Accident Tolerant Chromium Coated Zircaloy-4 Claddings,” *Top Fuel 2016 Boise ID Sept. 11-15 2016*, 2016.

[14] H.-G. Kim, I.-H. Kim, Y.-I. Jung, D.-J. Park, J.-Y. Park, and Y.-H. Koo, “Adhesion property and high-temperature oxidation behavior of Cr-coated Zircaloy-4 cladding tube prepared by 3D laser coating,” *J. Nucl. Mater.*, vol. 465, pp. 531–539, Oct. 2015.

[15] R. Van Nieuwenhove, V. Andersson, J. Balak, and B. Oberländer, “In-Pile Testing of CrN, TiAlN, and AlCrN Coatings on Zircaloy Cladding in the Halden Reactor,” in *Zirconium in the Nuclear Industry: 18th International Symposium*, 2018.

[16] B. Maier *et al.*, “Development of Cold Spray Coatings for Accident-Tolerant Fuel Cladding in Light Water Reactors,” *JOM*, Nov. 2017.

[17] J. C. Brachet *et al.*, “CEA studies on advanced nuclear fuel claddings for enhanced Accident Tolerant LWRs Fuel (LOCA and beyond LOCA conditions),” *Contrib Mater Investig Oper Exp LWRs’ Saf. Perform Reliab Fr Avignon*, 2014.

[18] A. S. Kuprin *et al.*, “Vacuum-arc chromium-based coatings for protection of zirconium alloys from the high-temperature oxidation in air,” *J. Nucl. Mater.*, vol. 465, pp. 400–406, Oct. 2015.

[19] Y. Wang *et al.*, “Behavior of plasma sprayed Cr coatings and FeCrAl coatings on Zr fuel cladding under loss-of-coolant accident conditions,” *Surf. Coat. Technol.*, vol. 344, pp. 141–148, Jun. 2018.

[20] F. P. Ford, B. M. Gordon, and R. M. Horn, “Corrosion in boiling water reactors,” *ASM Handb.*, vol. 13, p. 341, 2006.

[21] G. Brun, J. Pelchat, J. Floz, and M. Galimberti, “Cumulative Fatigue and Creep-Fatigue Damage at 350°C on Recrystallized Zircaloy-4,” in *Zirconium in the Nuclear Industry*, R. Adamson and L. Van Swam, Eds. 100 Barr Harbor Drive, PO Box C700, West Conshohocken, PA 19428-2959: ASTM International, 1987, pp. 597-597–20.

[22] X. Lin and G. Haicheng, “Low cycle fatigue properties and microscopic deformation structure of Zircaloy-4 in recrystallized and stress-relieved conditions,” *J. Nucl. Mater.*, vol. 265, no. 1, pp. 213–217, Feb. 1999.

[23] A. Soniak, S. Lansiart, J. Royer, J. Mardon, and N. Waeckel, “Irradiation Effect on Fatigue Behavior of Zircaloy-4 Cladding Tubes,” in *Irradiation Effect on Fatigue Behavior of Zircaloy-4 Cladding Tubes*, 1994.

[24] “The fatigue behaviour of α-zirconium and Zircaloy-2 in the temperature range 20 to 700° C,” *J. Nucl. Mater.*, vol. 67, no. 1–2, pp. 215–228, Jun. 1977.
[25] S. L. Dickerson and J. C. Gibeling, “Low cycle fatigue of niobium–zirconium and niobium–zirconium–carbon alloys,” *Mater. Sci. Eng. A*, vol. 278, no. 1, pp. 121–134, Feb. 2000.
[26] P. Pankaskie, “Fatigue-Crack Growth and Propagation in 2.5Nb Zirconium Alloy Pressure Tubing,” in *Fatigue-Crack Growth and Propagation in 2.5Nb Zirconium Alloy Pressure Tubing*, 1969.
[27] H.-G. Kim, J.-H. Yang, W.-J. Kim, and Y.-H. Koo, “Development Status of Accident-tolerant Fuel for Light Water Reactors in Korea,” *Nucl. Eng. Technol.*, vol. 48, no. 1, pp. 1–15, Feb. 2016.
[28] A. Moridi, S. M. Hassani-Gangaraj, S. Vezzú, L. Trško, and M. Guagliano, “Fatigue behavior of cold spray coatings: The effect of conventional and severe shot peening as pre-/post-treatment,” *Surf. Coat. Technol.*, vol. 283, pp. 247–254, Dec. 2015.
[29] T. S. Price, P. H. Shipway, and D. G. McCartney, “Effect of cold spray deposition of a titanium coating on fatigue behavior of a titanium alloy,” *J. Therm. Spray Technol.*, vol. 15, no. 4, pp. 507–512, Dec. 2006.
[30] P. Cavaliere *et al.*, “Microstructural and fatigue behavior of cold sprayed Ni-based superalloys coatings,” *Surf. Coat. Technol.*, vol. 324, pp. 390–402, Sep. 2017.
[31] P. Cavaliere and A. Silvello, “Fatigue behaviour of cold sprayed metals and alloys: critical review,” *Surf. Eng.*, vol. 32, no. 9, pp. 631–640, Sep. 2016.
[32] ASTM International, West Conshohocken, PA, “ASTM B614-16 Standard Practice for Descaling and Cleaning Zirconium and Zirconium Alloy Surfaces,” 2016.
[33] I. D. Peggs and D. P. Godin, “The yield strength-hot hardness relationship of Zircaloy-4,” *J. Nucl. Mater.*, vol. 57, no. 2, pp. 246–248, Aug. 1975.
[34] K. G. Field, M. A. Snead, Y. Yamamoto, and K. A. Terrani, “Handbook on the Material Properties of FeCrAl Alloys for Nuclear Power Production Applications,” 2017.
[35] S. Chen and C. Yuan, “Neutronic Analysis on Potential Accident Tolerant Fuel-Cladding Combination $U_3Si_2$-FeCrAl,” *Sci. Technol. Nucl. Install.*, vol. 2017, pp. 1–12, 2017.
[36] H. GRUPPELAAR, “EVALUATED NEUTRON CROSS SECTIONS OF NATURAL MOLYBDENUM,” p. 54.
[37] M. Chadwick *et al.*, “ENDF/B-VII. 1 nuclear data for science and technology: cross sections, covariances, fission product yields and decay data,” *Nucl. Data Sheets*, vol. 112, no. 12, pp. 2887–2996, 2011.
[38] H. Shah *et al.*, *Development of Surface Coatings for Enhanced Accident Tolerant Fuel (ATF)*. 2017.
[39] “Standard Test Method for Flexural Strength of Advanced Ceramics at Ambient Temperature,” ASTM International, 2013.
[40] ASTM International, “Standard Test Method for Measurement of Fatigue Crack Growth Rates,” 2011.
[41] M. Wagih, Y. Che, and K. Shirvan, “Fuel Performance of Multi-Layered Zirconium Based Accident Tolerant Fuel Cladding,” in *ICAPP*, 2017.